Coupon scale Z-pinned IM7/8552 delamination tests under dynamic loading

Hao Cui[a,c,1], Yusuf Mahadik[b], Stephen R. Hallett[b], Ivana K. Partridge[b], Giuliano Allegri[b], Sathiskumar A Ponnusami[c] , Nik Petrinic[c]

[a]School of Aerospace, Transport and Manufacture, Cranfield University,Cranfield, UK

[b]Advanced Composites Centre for Innovation and Science (ACCIS), University of Bristol, Bristol, UK

[c]Department of Engineering Science, University of Oxford, Oxford, UK

Abstract

Dynamic impact onto laminated composite structures can lead to large-scale delamination. This can be mitigated by the introduction of through-thickness reinforcement, such as z-pins. Here, mode I & II and mixed-mode delamination tests have been designed and conducted at high loading rate, for both unpinned and Z-pinned coupons to study the effect of rate of loading. It was found that the Z-pins were not effective in delaying the dynamic crack initiation or resisting the dynamic propagation of delaminations shorter than 5 mm. However, the further growth of cracks was substantially delayed by Z-pinning, especially for the pure mode I and mode I dominated failure modes. On the other hand, the effectiveness of Z-pins in shear tests was relatively modest. The mode I dominated delamination resistance of Z-pinned laminates was found to be sensitive to the loading rate.

Keywords

Through-thickness reinforcement; Delamination; Fracture Mechanics;

[1] Corresponding author: Email: hao.cui@cranfield.ac.uk;
Phone: +44(0)1234754454

1. Introduction

Laminated composites are widely employed in aerospace structures [1,2], thanks to the high strength and stiffness of carbon fibre reinforcement. However, inter-laminar delamination damage still represents a major concern for the integrity of composites structures [3–5], especially under impact loading [6–9]. Through-thickness reinforcement (TTR) in the form of Z-pins, i.e. metallic or composite rods orthogonally inserted with respect to the laminate mid plane [10], has been employed for improving the inter-laminar performance of fibre-reinforced composite stacks [11].

Standard delamination experiments have been conducted to characterize the contribution of Z-pinning to delamination resistance. The mode I delamination fracture toughness for crack initiation in double cantilever beam (DCB) tests is not affected by Z-pinning, while it is considerably increased during the delamination propagation stage [12–14]. In end notched flexure (ENF) tests, Z-pinning was also reported to be effective only at resisting delamination propagation [11,13,15]. Most research on the delamination behaviour of Z-pinned composites has been conducted at quasi-static loading rates. However, despite the fact that Z-pinning has been employed for improving impact-damage resistance, the resulting dynamic effects are still not fully understood. Recently, ENF tests have been conducted at displacement rates up to 5m/s [16]. It was reported that the delamination resistance at the moment of crack initiation was significantly improved with Z-pinning, and this effect became more pronounced as the loading rate was increased.

The effect of Z-pins on the initiation and growth of delamination is largely dominated by the bridging response of individual TTR rods, and the improvement provided by Z-pins to the delamination resistance is essentially attributed to the energy dissipation occurring during the pin progressive pull out and/or failure. The former prevails in mode I delamination, whereby the pull-out displacement can be as high as half of the laminate thickness [10,13,17,18].

However, Z-pins cannot arrest crack initiation, as the energy dissipation associated to the Z-pin debonding process from the embedding laminate is usually negligible [19], and relatively large crack opening displacements need to be attained before the energy dissipation due to frictional pull-out becomes significant. In mode II dominated regimes the Z-pins typically fail [20,21]; the bridging force provided by Z-pins increases almost linearly with the sliding displacement of the delamination faces [19], and it falls suddenly as the TTR rods experience failure. The Z-pin response also shows significant dependency on the loading rate, especially in mode I dominated conditions [19]. The response of individual Z-pin under dynamic loading has been characterized over the full range of mode-mixity ratio [22]. The experimental evidence clearly showed the progressive transition from complete pull-out to Z-pin failure delamination as the testing conditions were progressively varied from mode I to mode II.

The bridging response of individual Z-pin has been investigated quite comprehensively, in both quasi-static conditions [17,21] and across a wide range of dynamic loading [19,22]. The delamination of Z-pinned composite laminates has been characterised using DCB and ENF samples under quasi-static regimes [12,13,15], with dynamic ENF tests reported in [16]. In this work, the dynamic delamination of Z-pinned laminates has been investigated systemically for the first time to cover a wide variety of loading modes at coupon (structural) scale, including pure mode I, pure mode II and mixed-mode. This aims to reveal the role of Z-pins interacting with a dynamically propagating delamination crack, which is beyond what can be determined from 'single pin' tests from previous work [19,22].

2. Experiments

2.1. Experimental setup

Delamination experiments on Z-pinned composite laminates were conducted under dynamic loading in this work. Further quasi-static and unpinned tests were conducted as well, in order to provide a benchmark for quantifying the influence of Z-pinning and rate on the delamination behaviour of composites laminates. The wedge-opened double cantilever beam (WDCB) test[23], the end notched flexure (ENF) test[24] and the single leg bending (SLB) test [25]were used for characterizing the mode I/II and mixed mode delamination behaviour in high loading rate (see Fig. 1). A split Hopkinson pressure bar (SHPB) system was used to apply a prescribed displacement to composite samples at striker velocity of around 4 m/s. The SHPB is made with 20 mm diameter titanium bars with elastic modulus of 105 GPa. A 1 mm thick rubber sheet was used as pulse shaper to generate the smooth rising edge of the indenter velocity, aiming to minimize the inertia effect due to the fixture and the coupons. Some WDCB tests were also conducted at displacement rate of around 7m/s. The dynamic test configurations shown in Fig.1 were also used for quasi-static experiments; a Zwick Roel 250 screw-driven testing machine was used to load the samples at a displacement rate of 0.01mm/s. The applied force was recorded with the test machine loading cell.

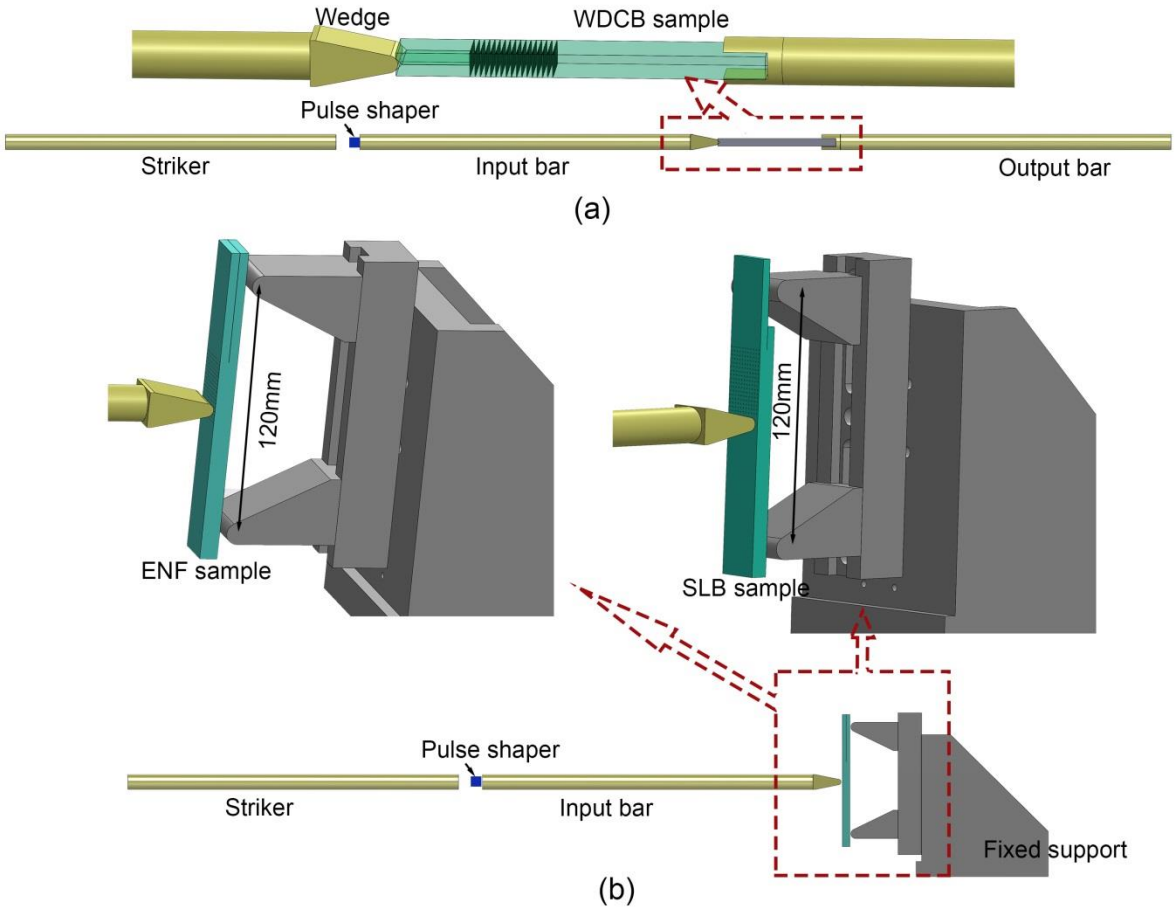

Fig.1. (a) Test setups for dynamic WDCB tests;(b) dynamic ENF and SLB tests

2.2. Specimen preparation

The composite samples were made with IM7/8552 unidirectional prepreg supplied by Hexcel in UK. These comprised 64 plies in total with the stacking sequence of $[[0/45/0/-45]_{4s}]_s$, resulting in a nominal thickness of 8mm. This 0° dominated layup was chosen to maximum the bending stiffness of the samples, and the ±45° layers provided enhanced lateral constraint for Z-pins in the crack propagation direction, similarly to quasi-isotropic laminates[19] as used in many current engineering applications. A 13 μm thick PTFE film was placed along part of the mid-plane of the laminates for creating a pre-crack. There were two 0° layers next to the PTFE film for preventing the out-of-plane migration of the interlaminar delamination.

The configuration of Z-pinned samples is illustrated in Figure 2. 0.28mm diameter carbon-fibre/BMI Z-pins with a relative spacing of 1.75mm were inserted in front of the initial crack tip; the aforementioned relative distance corresponds to a 2% of Z-pin areal density. The Z-pin insertion method has been introduced in previous publication[19]. The distance between the first pin row and the edge of the PTFE film was measured to be less than 2mm, such that the Z-pins should be involved in the crack initiation process. No further pre-cracking method was used in this study, for the purpose of avoiding any permanent change to the pin/laminates interface prior to tests, as well as damage in the Z-pins. The nominal width of the samples was 19.25mm, with 11 pins along the width direction. There were 17 pins in the length direction, providing a sufficient gauge length for the propagation of delamination crack in the Z-pinned zone. V-notches were machined at the edge of the WDCB samples, in order to accommodate the initial wedge penetration into the coupons. Unpinned samples were prepared for each type of tests with the same nominal geometry as Z-pinned ones.

A strain gauge attached on the back of the laminates, as illustrated in Fig.2, was used to monitor the bending strain, and then classical beam theory was used to estimate the applied force. The bending stiffness of the laminates was assumed to be independent of the loading rate in this study, as the elastic modulus of multi-directional laminates didn't show noticeable dependence on strain rate[26,27] .

The side surface of the samples was painted white to facilitate the observation of the crack tip position. Black speckles were sprayed on top, enabling the analysis of deformation via digital image correlation (DIC). A detailed introduction to the DIC process used here can be found in previous work [26]. A Specialised Imaging Kirana ultra-fast video camera with a resolution of 924×768 pixels was used in the dynamic experiments for recording the sample

images at a frame rate of 100,000 – 500,000 FPS, depending on the duration of the failure event. For the quasi-static experiments a USB camera fitted to the ZWICK testing machine was used to capture the deformation of samples at a frame rate of 1 FPS.

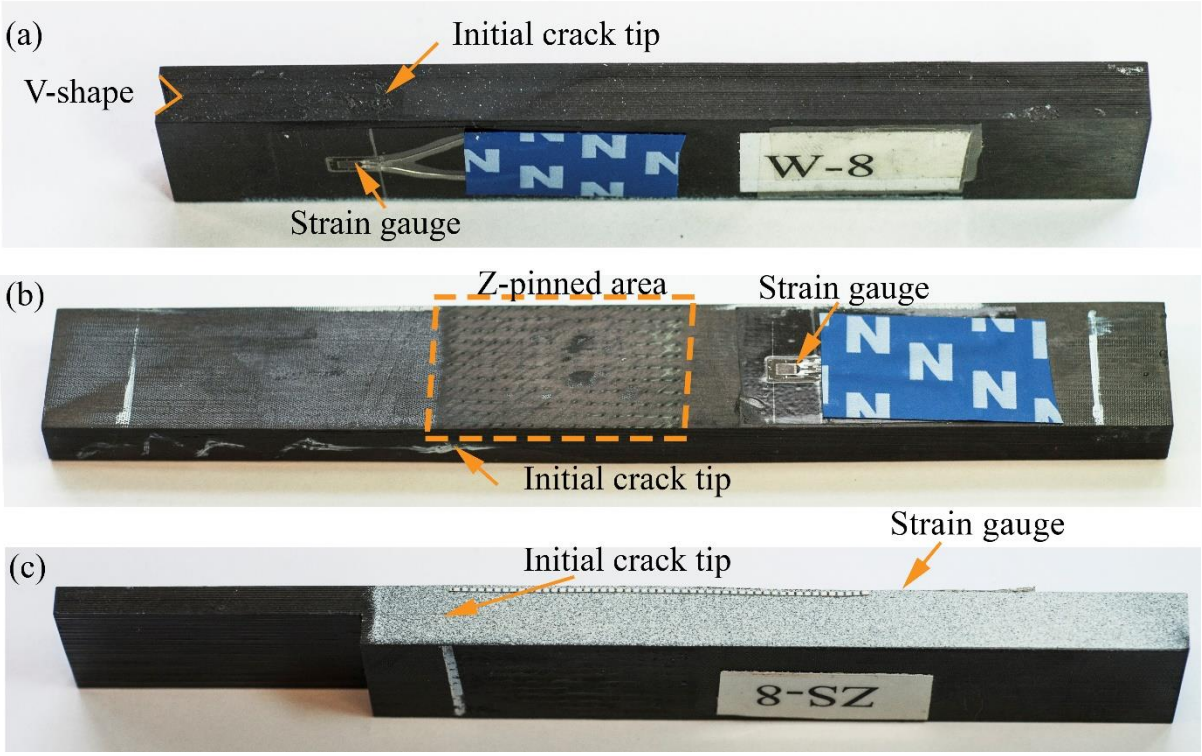

Fig.2 Design of Z-pinned laminates for (a) WDCB,(b) ENF and (c) SLB tests

2.3. Data processing

The Z-pins provide bridging forces that close the delamination for a considerable distance in the interlaminar crack tip wake [13]. The presence of a large bridging zone that develops behind the crack tip may invalidate traditional data reduction methods based on linear elastic fracture mechanics (LEFM). Therefore, it is challenging to evaluate the delamination fracture toughness of Z-pinned laminates, especially in the crack propagation stage. Besides, the monitoring of crack length during experiments can be difficult, as the crack may remain closed in mode II dominated cases [28]. The presence of Z-pins in the wake of the crack tip also makes it questionable to employ the “nominal” crack length in LEFM-based data reduction methods [29,30]. Methods based on the J-integral have been proposed to get the fracture toughness of adhesive bonds [31,32]. In these approaches, instead of measuring the

crack length during experiments, the deformation of adherends near the initial crack tip needs to be monitored. The delamination of laminates is very similar to the debonding process in adhesive joints, as the damage is confined within a thin strip, and the data reduction techniques developed for adhesive joints undergoing dis-bond may be adopted to estimate the delamination fracture toughness.

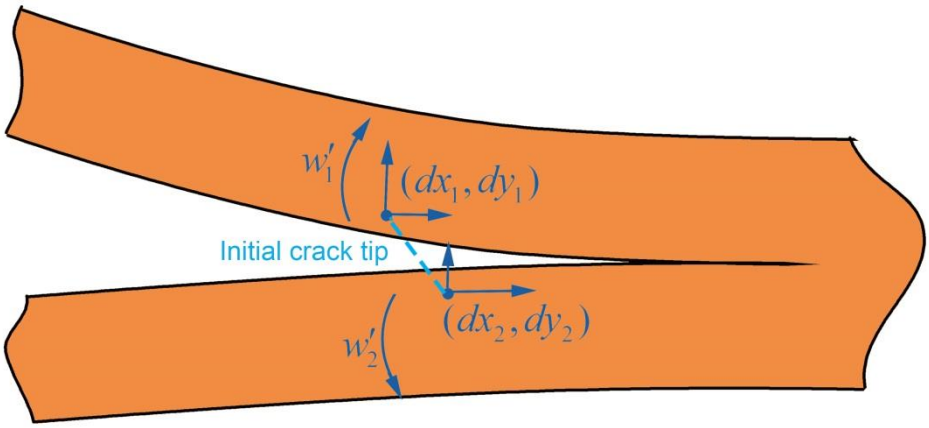

Fig.3 Illustration of displacement near the initial crack tip

The mode I fracture toughness can be calculated as [32]:

$$G_{\mathrm{I}} = \frac{12P^2a_0^2}{Eh^3b^2} + \left(w_1' - w_2'\right)P \tag{1}$$

where P is the applied load, E is the nominal flexural modulus of composite laminates, h is half of the sample thickness, a_0 is the initial crack length. The w_1' and w_2' are the rotation of the laminates near the initial crack tip, as illustrated in Fig.3.

The mode II fracture toughness is calculated as [31]:

$$G_{\mathrm{II}} = \frac{9P^2a_0^2}{16Eh^3b^2} + \frac{3Pv}{8bh} \tag{2}$$

where v is the relative shear displacement of the laminates at the initial crack tip.

The deformation at initial crack tip illustrated in Fig.3, was obtained with high-speed camera and the DIC method. The displacement near initial crack tip was calculated as:

$$\delta = dy_1 - dy_2 \tag{3a}$$

$$v = dx_1 - dx_2 \tag{3b}$$

in which δ is the opening and v is the shear displacement. These relative displacements were measured at the edge of adherend in previous debonding experiments [32], as all fracture energy was dissipated within the bondline. The failure process zone is typically just 10 μm thick in composite laminates [33,34], making it challenging to get an accurate measurement of δ and v in practice. As illustrated in Fig.3, the shear displacement was measured at the location around 0.5mm from the delamination interface. Considering the fact that composite material outside failure process zone (FPZ) remain elastic, the error involved in the measurement should be relatively small. Because of these approximations, the fracture toughness values presented in this work may only be regarded as "apparent" values, which provide a metric for comparison among the various coupon configurations considered here, but do not represent an actual material property.

The SLB test was considered as the superposition of DCB and ENF samples as shown in Fig.4. The force components for mode I and mode II components can be calculated as:

$$P_{\mathrm{I}} = F/4 \tag{4a}$$

$$P_{\mathrm{II}} = F \tag{4b}$$

The energy dissipations can be calculated as:

$$J_{\mathrm{I}} = \frac{9a_0^2 P_{\mathrm{I}}^2}{E_f h^3 b^2} + \frac{P_{\mathrm{I}}}{b}\left(w_1' - w_2'\right) \tag{5a}$$

$$J_{\mathrm{II}} = \frac{9a_0^2 P_{\mathrm{II}}^2}{16E_f h^3 b^2} + \frac{3vP_{\mathrm{II}}}{8bhL} \tag{5b}$$

The superposition theory is strictly valid only for purely linear elastic fracture problems, which is not the case here due to the inevitable nonlinear large-scale bridging provided by Z-pins. Although the accurate fracture toughness may not be obtainable, the apparent value estimated from the method considered here should at least reflect the efficiency of Z-pinning on improving the resistance to delamination damage.

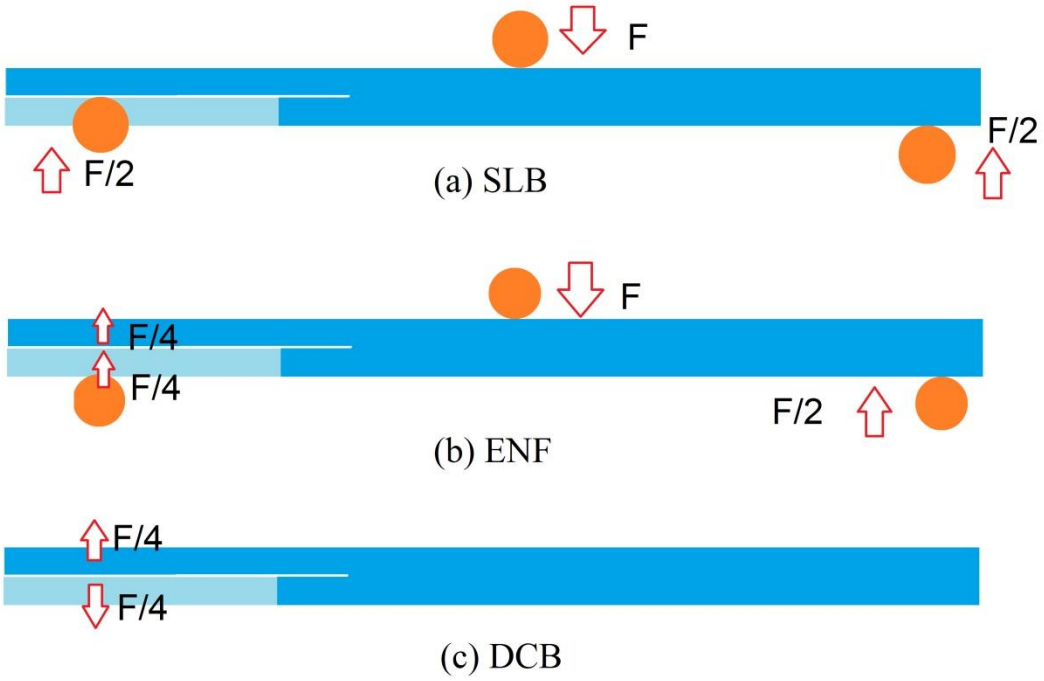

Fig.4 The superposition theory for SLB analysis, (a) the SLB test as composition of (b) ENF test and (c) DCB test

3. Results

3.1 Mode I

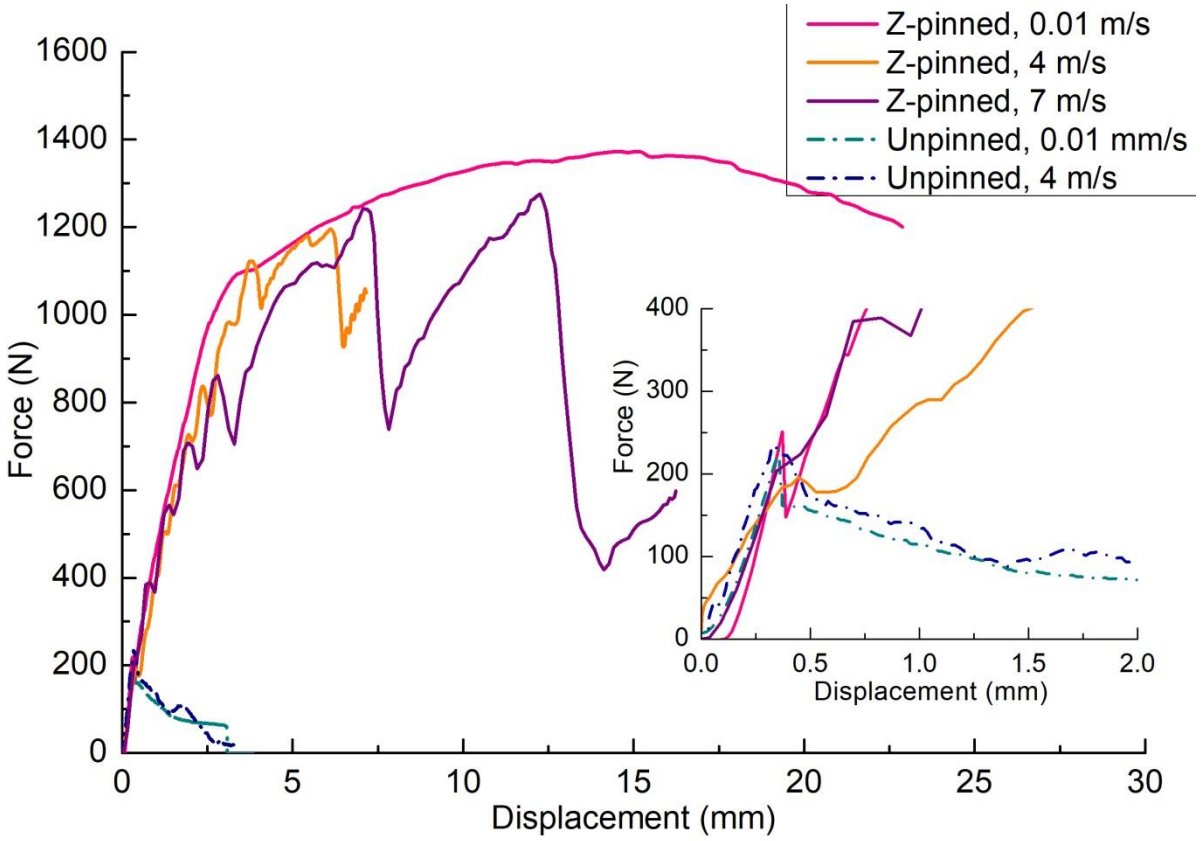

Fig.5 Typical force-displacement curves for WDCB tests

The lateral force responsible for opening the WDCB sample was calculated using the strain signal on the back of the laminates, which is plotted as function of the wedge displacement in Fig.5. The force dropped at around 0.2 mm for all samples because of crack onset. The force kept decreasing with further displacement of the wedge in unpinned samples, while increased considerably for the Z-pinned ones. The displacement required for the complete failure of Z-pins was so high that it could not be achieved within a single pulse from the SHPB striker. Inevitably, the displacement is not applied at constant rate, which resulted in considerable oscillations on the dynamic response curves. In general, the Z-pinned samples exhibited a higher loading capacity in the quasi-static tests than that in the dynamic cases. The failure load of unpinned samples showed little dependence on the loading rate.

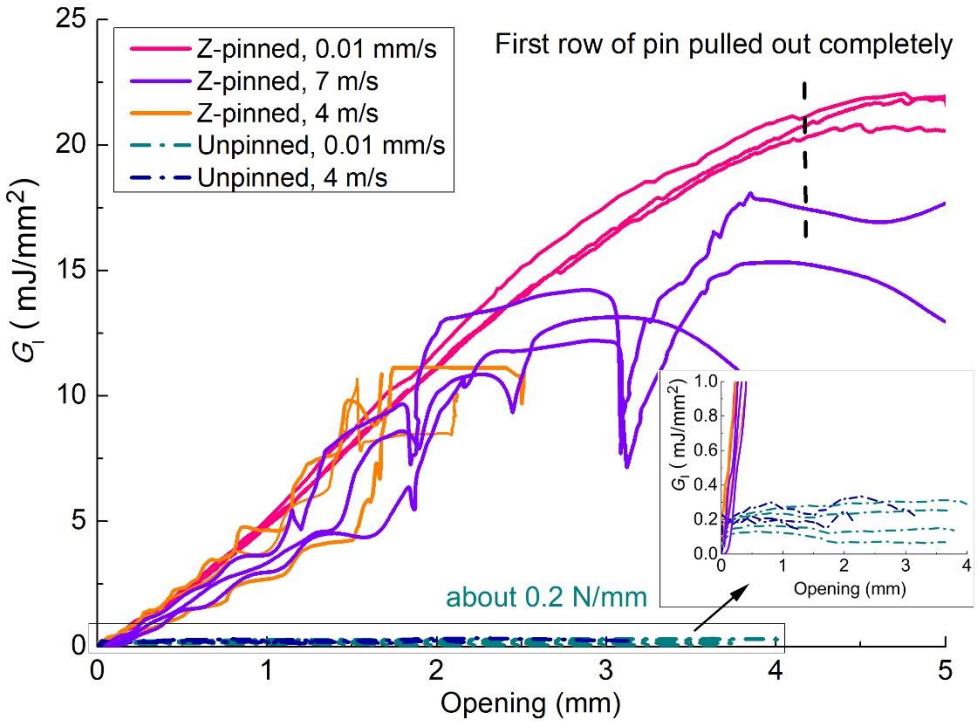

Fig.6 Mode I delamination fracture toughness

The mode I delamination fracture toughness calculated using Eq (1) is shown in Fig.6, where an improved resistance to crack propagation can be observed for the Z-pinned coupons. The opening displacement near the initial crack tip was analysed with DIC methods; this displacement also corresponds to the pull-out distance of the first row of Z-pins, as illustrated in Fig.1. The delamination toughness of unpinned laminates did not change much with loading rate, and plateaued at around 0.2N/mm, a value similar to that reported in [35]. In the Z-pinned samples, the fracture toughness kept increasing until the first row of Z-pins was completely pulled out. The G_{IC} was increased by more than 100 times the unpinned value, in the quasi-static tests. Under dynamic conditions, the Z-pinned samples performed similarly to the TTR coupons tested in quasi-static conditions, but with considerably more variability, and decrease in measured fracture toughness in the latter stages of z-pin pullout.

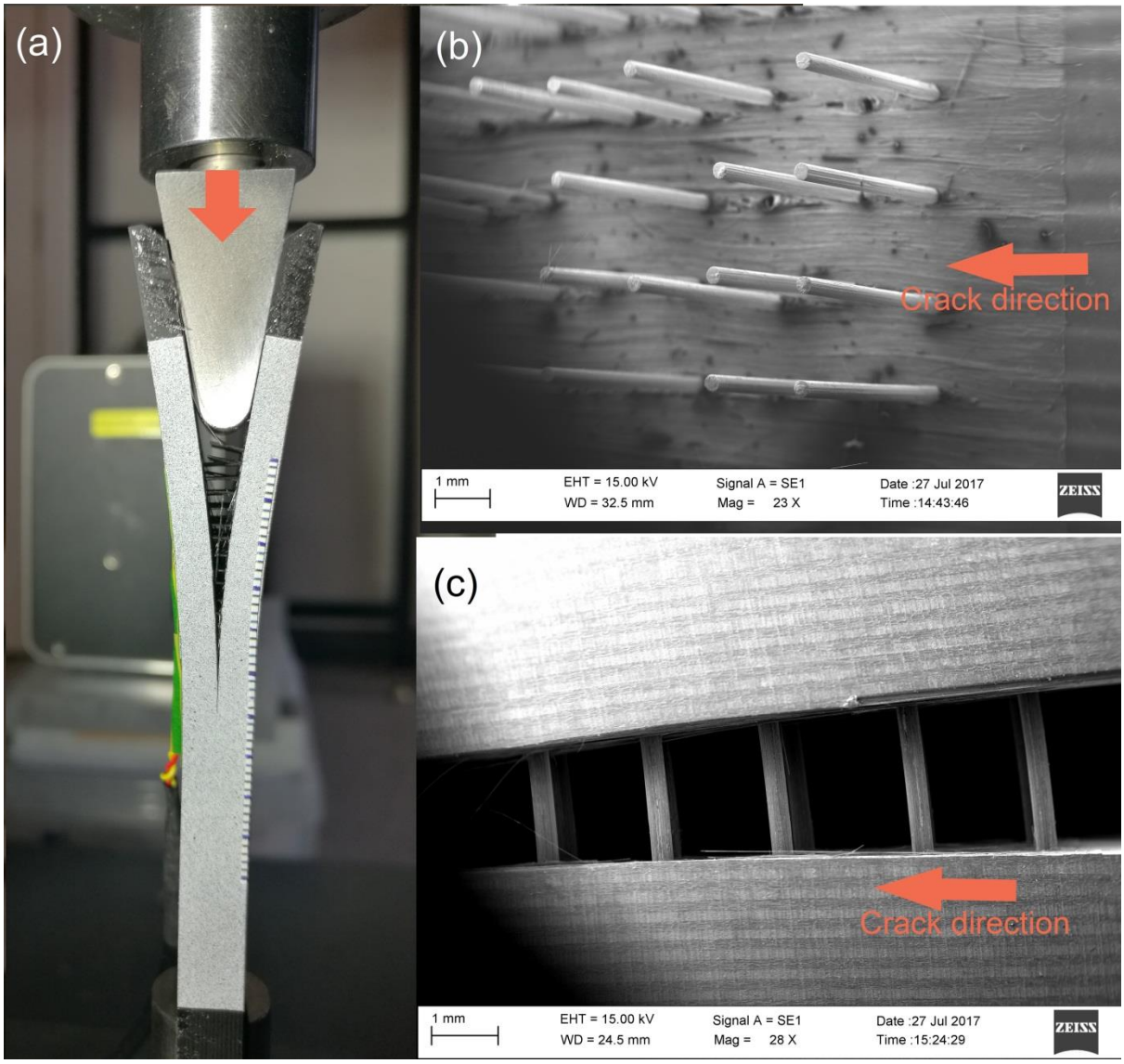

Fig.7. Failure modes in Z-pinned WDCB sample (a) the failure modes in WDCB samples at quasi-static loading rate; (b) the failure surface of quasi-static sample; (c) the side view of a dynamic sample

A Z-pinned sample tested under quasi-static conditions is shown in Fig.7a. Although some pins near the initial crack tip have been pulled out completely, the crack propagated for less than 30mm. The comparison of pin response in quasi-static and dynamic tests is shown in Fig. 7b&c. The behaviour of individual Z-pins did not show any significant dependence on the loading rate, as all pins were debonded and then gradually pulled out with the increase in wedge displacement.

3.2 Mode II

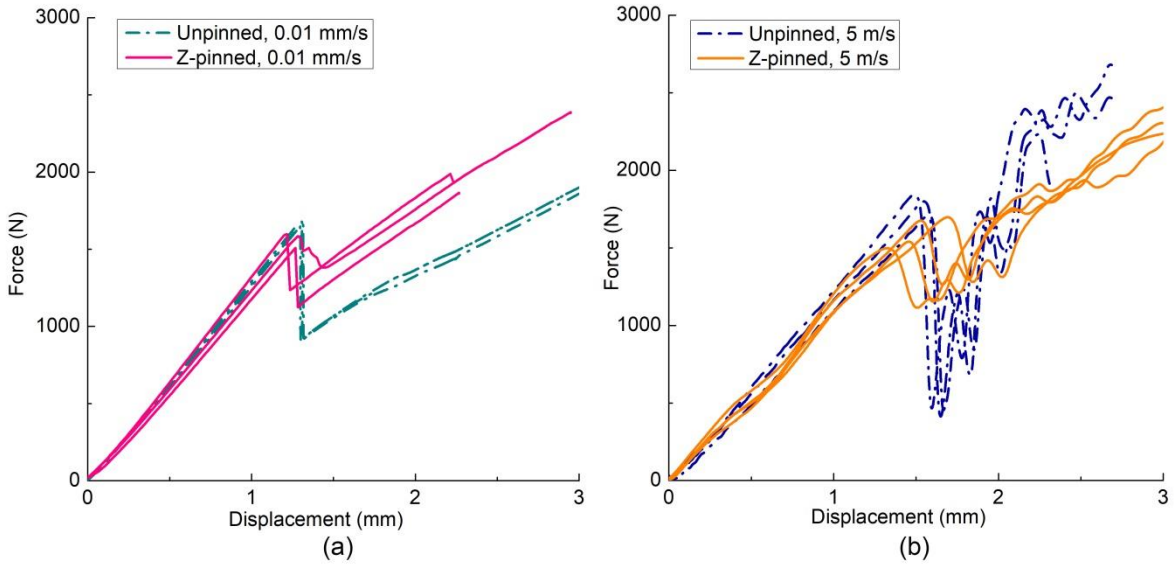

Fig.8 Force-displacement curves in ENF tests

The force-displacement curves from ENF tests are presented in Fig.8. Although pins were placed very close to the initial crack tip, the force corresponding to crack initiation was unaffected by the presence of TTR. At the loading rate of 0.01mm/s, all unpinned samples and two out of three Z-pinned samples experienced an initial unstable crack growth. The delamination propagation became stable after the interlaminar crack had grown beyond the half the coupon gauge length (i.e. crack propagation of more than 25mm). The only noticeable difference between un-pinned and Z-pinned coupons in quasi-static test conditions is that the residual force after the unstable crack propagation phase is increased for the coupons with TTR. The crack initiation load was also insensitive to the presence of Z-pins in the dynamic experiments. However, the oscillations in the dynamic response of unpinned samples were more significant than that in the Z-pinned ones, because the TTR rods helped preserve the loading capacity after the initial unstable crack propagation.

The mode II delamination fracture toughness is plotted as function of the shear displacement at the initial crack tip in Fig.9. The energy level estimated via the J-integral ramped up linearly with the shear displacement until crack onset. The critical fracture toughness for the delamination initiation is unaffected by Z-pinning and it was also found to

be independent from the loading rate. The critical fracture toughness ranged between 0.9 and 1.25N/mm for all samples. The fracture toughness dropped rapidly due to the unstable crack growth process, which also resulted in the straight horizontal lines in Fig.9, due to a lack of data points. In general, Z-pinned samples exhibited higher delamination resistance than unpinned ones.

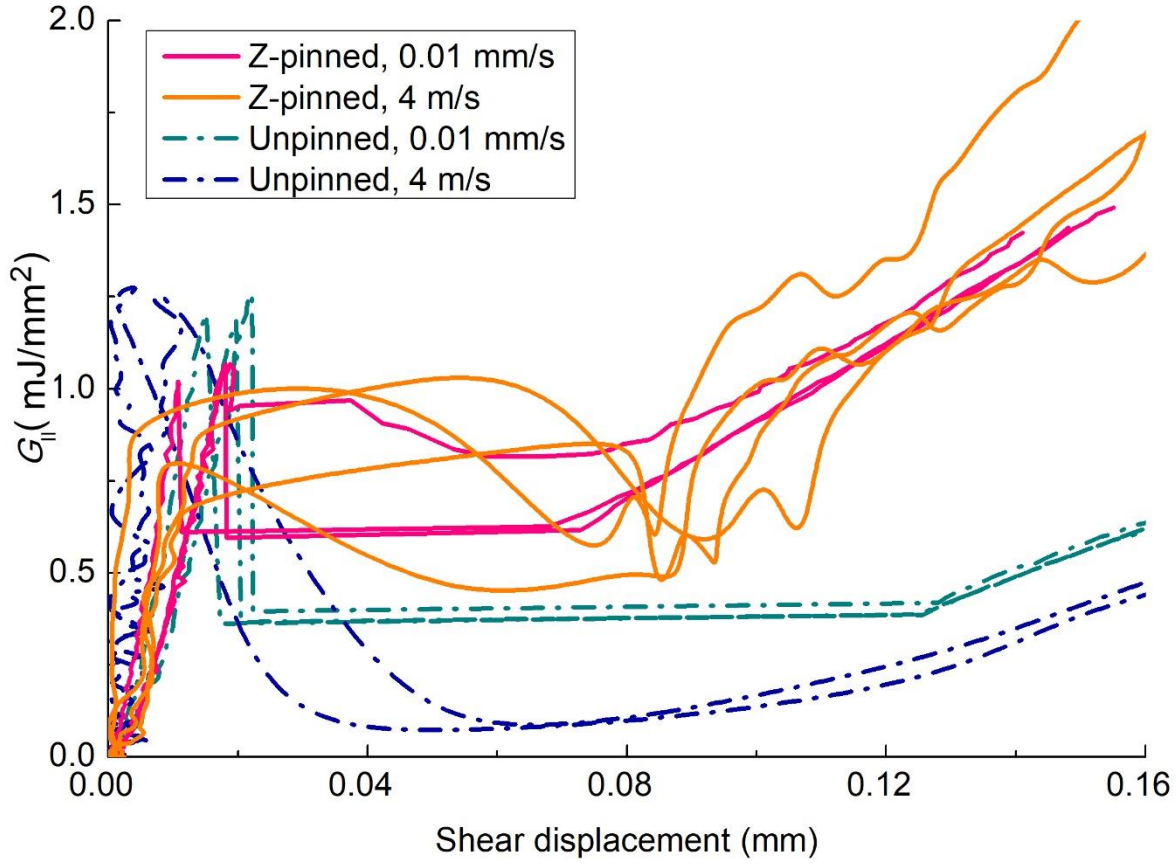

Fig.9 The mode II delamination fracture toughness from ENF tests

The quasi-static ENF tests were stopped after cracks have grown for longer than 30 mm. The edge of one Z-pinned sample was polished until pins were revealed, and analysed with /optical microscopy, as shown in Fig.10. The shear crack initiating from the tip of the release film was clearly visible. However, all Z-pins (including the first TTR rod in front of the crack tip) remained intact, without any noticeable internal splitting. Only some debonding between

the pins and the embedding laminate was observed near the delamination surface. The bending of Z-pins has caused residual plastic deformation of the surrounding epoxy [18], as highlighted by the circles in Fig.10.

The Z-pins in the ENF samples were ruptured very close to the delamination surface in dynamic tests, as shown in Fig.11, similarly to the single pin shear failure mode reported in [19]. Since the shear behaviour of the single Z-pins did not show significant dependency on the loading rate [19], and the response of unpinned laminates was also found to be independent from the loading rate (as illustrated in Fig.9), it can be speculated that Z-pin failure happened at a much later stage than the crack onset.

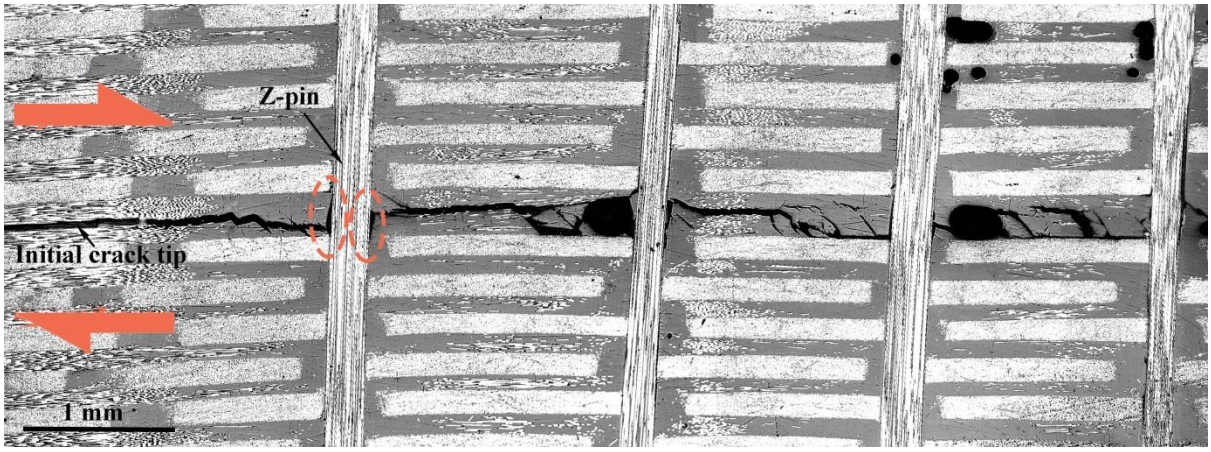

Fig.10 Side view micrograph of Z-pinned samples from quasi-static ENF tests, with the residual plastic deformation of surround matrix highlighted

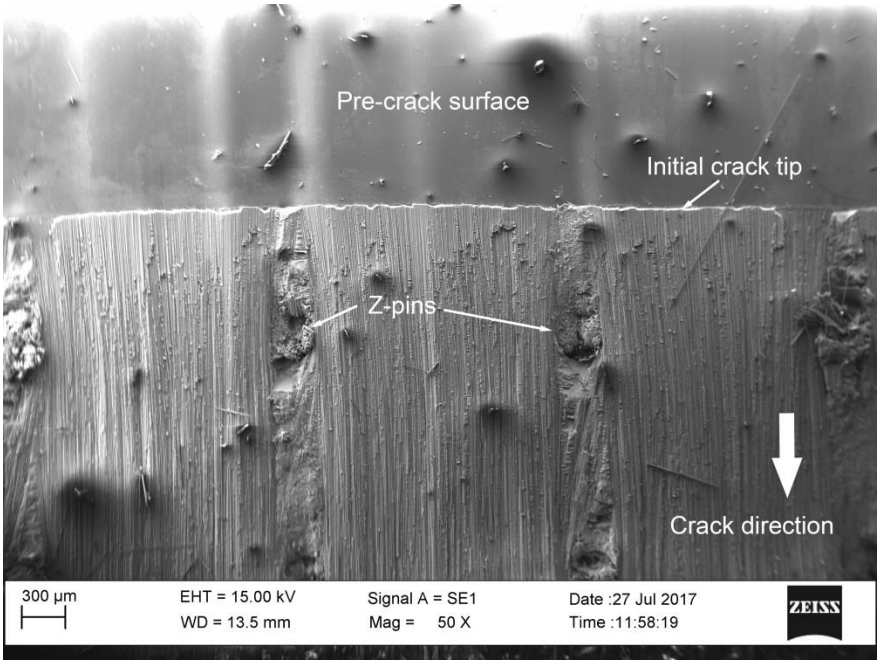

Fig.11 Failure surface of Z-pinned samples form dynamic ENF tests

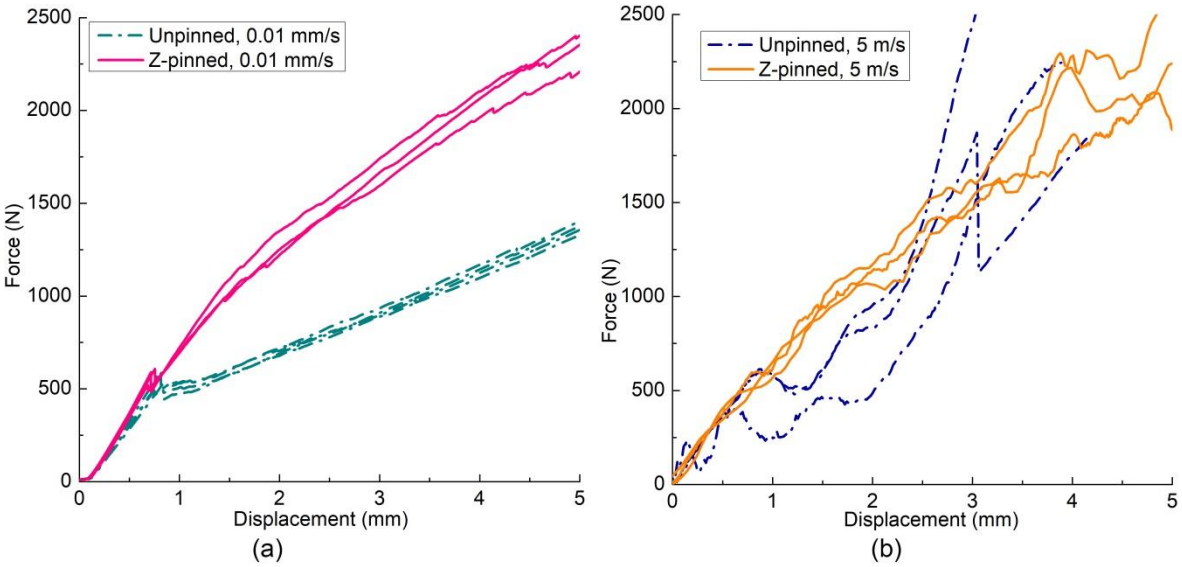

Fig.12 Force displacement curves from SLB tests

3.3 Mixed mode

The force-displacement curves from SLB tests are presented in Fig.12. Similarly to the mode I&II results obtained with WDCB and ENF tests (See Fig.5&8), the load that corresponded to crack onset was not influenced by either the presence of Z-pining or the applied displacement rate. One of the force versus displacement traces for an unpinned sample tested in dynamic conditions exhibits significant oscillations. This test was conducted

without using the pulse shaper and this caused significant vibrations. The crack propagation was very stable in SLB tests and Z-pinning significantly raised the loading capacity during delamination propagation. There was also a rapid increase of force in unpinned dynamic tests, which was caused by the delamination crossing the strain gauge position. The decreased bending stiffness of laminates resulted in an unusual ramping up of the strain signal, and the test measurement has become invalid beyond this point.

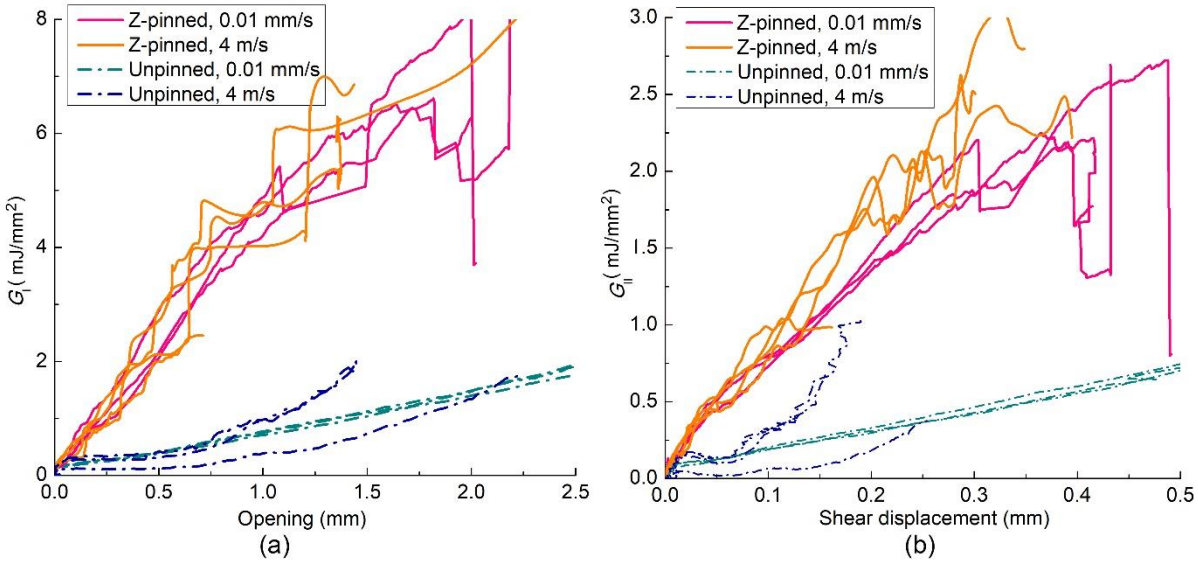

Fig.13 The fracture toughness-deformation at initial crack tip: (a) mode I component; (b) mode II component

The opening and shear displacement near the initial crack tip (illustrated in Fig.3) have been obtained using the DIC technique described above. The mode I&II fracture toughness components have been plotted in Fig.13. Once more, Z-pins were not effective in delaying the initiation of cracks, but they considerably improved the fracture toughness during the crack propagation stage. For the SLB configuration used here, the mode mix ratio $G_{II}/(G_I+G_{II})$ was around 0.3. Although the fracture toughness estimated with J-integral can only be regarded as the "apparent" value, the contribution of Z-pins to the mixed mode delamination resistance is quite evident and conclusive.

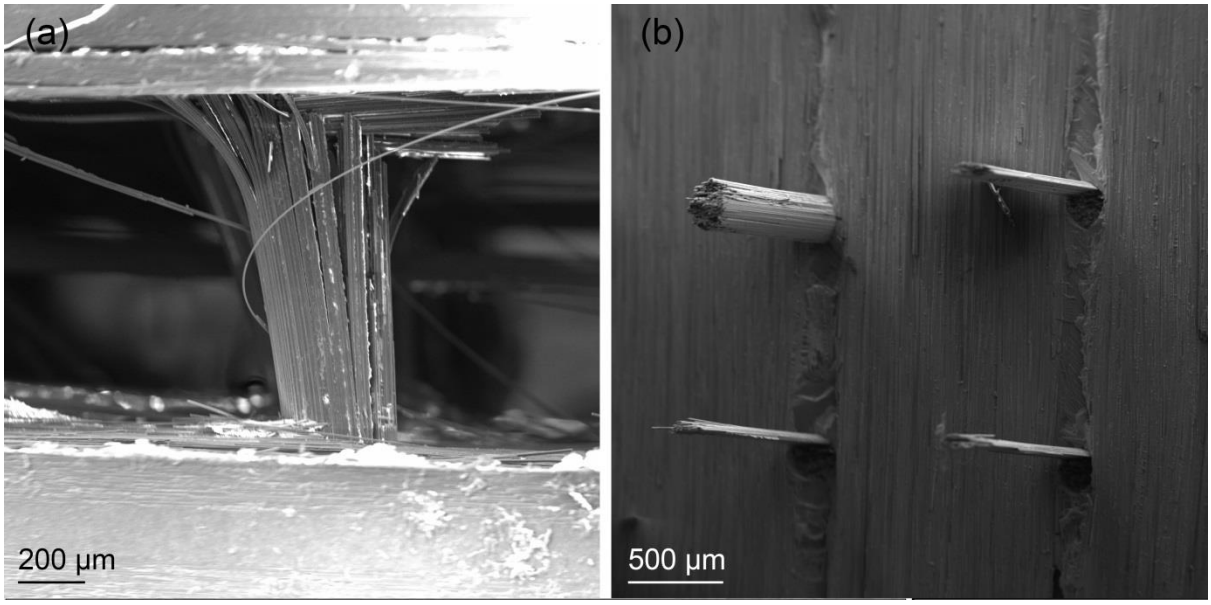

Fig.14. (a) the quasi-static failure of Z-pinned SLB sample; (b) the dynamic failure of Z-pinned SLB sample

In SLB tests, the Z-pins were first debonded from the surrounding laminates and then pulled out, as show in Fig.14. Splitting as well as fibre failure was also observed within individual Z-pins. These are caused by to the relative shear displacement of the laminate faces and the resulting bending moment applied on the Z-pins. No pins have been fully broken or pulled-out in the quasi-static tests, due to the premature failure of the coupon arms. However, all pins were ruptured with further increase of load in the dynamic tests; however, the failed pins were also partially pulled-out, as a clear reflection of the mixed-mode conditions achieved during the tests.

4. Discussion

4.1 Crack growth rate

The influence of Z-pinning on the force and apparent fracture toughness has been recorded for all tests discussed in the previous sections. It worth noting that the fracture toughness presented here may not reflect the actual delamination resistance of the laminates,

because of the large-scale fibre bridging that was observed in all tests affecting the calculations performed. Moreover, a further approximation was introduced by estimating the displacement near crack tip using DIC. However, it is clear that Z-pins did not improve the delamination fracture toughness at the crack onset. Nonetheless, the delamination resistance during the crack propagation stage for WDCB and SLB tests was considerably increased by the presence of Z-pins. This section aims to provide a detailed investigation on how individual Z-pins affect the propagation of delamination.

In Fig.15, the initial crack tip opening and the growth of pure mode I delamination cracks is plotted as a function of the wedge displacement for WDCB experiments. Compared with the unpinned results, the opening was suppressed by Z-pins. Delamination initiated at similar level of displacement for both the Z-pinned and unpinned coupons. The crack grew at an almost constant rate for unpinned samples, which was considerably delayed by Z-pins in both quasi-static and dynamic experiments.

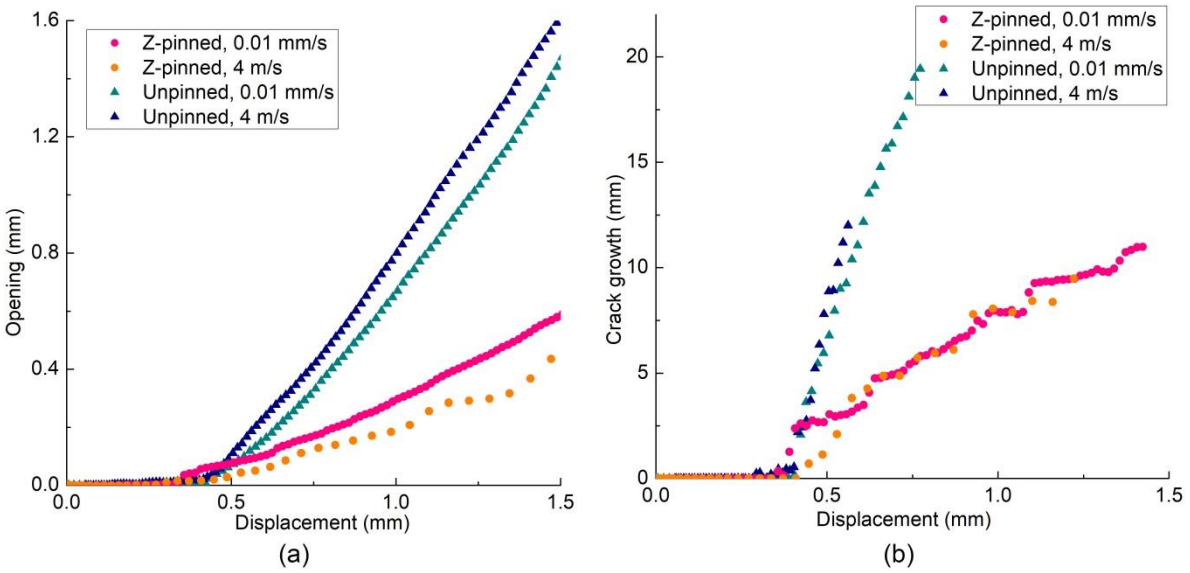

Fig.15 (a) the opening of initial crack tip and (b) the crack length with the displacement loading of wedge in WDCB experiments

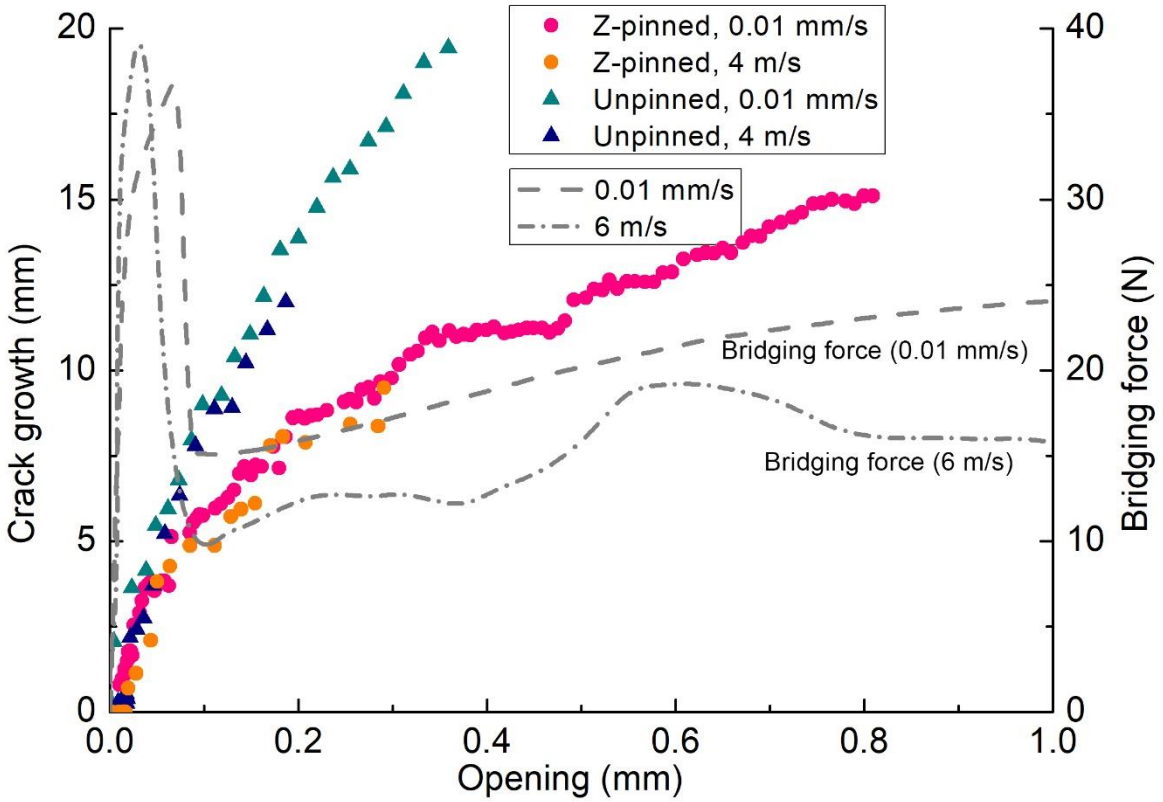

Fig.16. The mode I crack length and single pin bridging force [19] with the opening of the initial crack tip.

The crack growth history from WDCB experiment is plotted in Fig.16 as function of the opening at the initial crack tip location, which approximates the pull-out displacement of the Z-pin closest to the initial crack tip. The bridging response characterized from single pin tests is also shown in Fig.16. The crack growth for the first 5mm seemed not to be influenced by Z-pinning, and the Z-pins got debonded within the surrounding laminates during this stage of the response. The pins were gradually pulled out with a further increase in opening, and the bridging force due to pin-laminate friction is primarily responsible for the reduced delamination growth rate in Z-pinned laminates.

The effective separation near the initial crack tip in SLB tests, including both opening and shear displacement components, is shown in Fig.17a. The Z-pinning substantially reduced the relative deformation near the initial crack tip, indicating the level of crack bridging force

provided by pins. The crack growth history is presented in Fig.17b. Similar to the pure mode I tests, the crack growth behaviour was unaffected by both the presence of Z-pins and loading rate in the first 5 mm of propagation. Further growth of crack was retarded in Z-pinned coupons, and delamination propagation rate was quite similar between quasi-static and dynamic tests. There are quite a number of factors affecting the crack growth and its measurement in pinned specimens. The crack length can be difficult to measure, especially at longer lengths, when significant bridging has occurred. The pins can add specimen to specimen variance given that their exact placement in the laminate, angle of insertion and quality will all influence crack growth rate. Oscillations in the applied force in the dynamic case will affect the also affect crack growth rate. Given these factors it is not considered that the difference in the curves at the later stages of crack growth is significant.

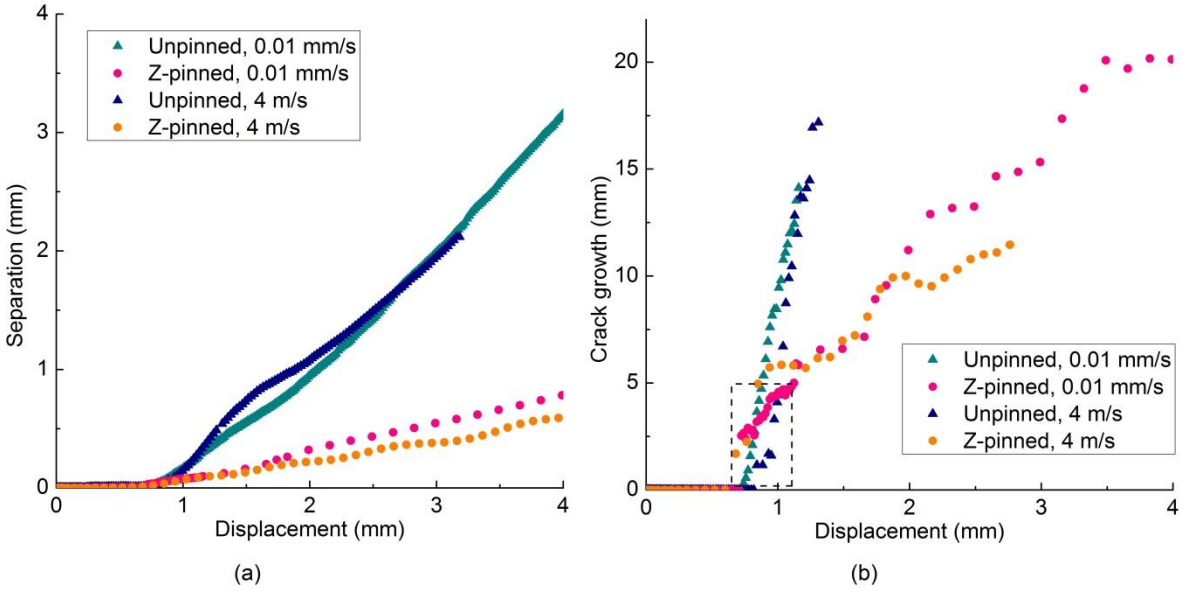

Fig.17. SLB test curves for (a) the separation at initial crack tip & (b) crack growth with the increase of displacement

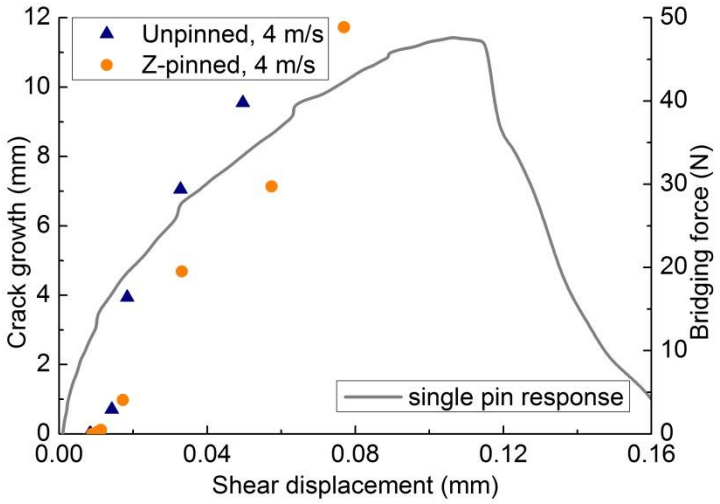

Fig.18. The crack length-shear displacement at initial crack tip in dynamic ENF tests, and single pin shear response [19]

The mode II delamination propagated unstably, which made crack length measurements particularly challenging during quasi-static ENF tests. The crack growth length was captured with a high-speed camera in dynamic ENF characterisations. The corresponding crack length is plotted in Fig.18, as function of the relative shear displacement, which approximates the actual sliding displacement experienced by Z-pins near initial crack tip. Crack initiated at the same level of sliding displacement for both unpinned and Z-pinned samples. Delamination propagated at slightly lower rate in Z-pinned samples than in those without pins. Single pin response in shear delamination was previously characterized [19], and it is also plotted in Fig.18. The TTR effectiveness in resisting crack propagation is not significant until the shear displacement reach about 0.1 mm, therefore , the crack had propagated for a considerable distance before considerable delamination retardation effect of the Z-pin kicked in. The effectiveness of Z-pins in dynamic shear delamination observed in the tests presented here was much lower than what previously reported [16]. This could be due to the fact that no pre-cracking from the PTFE film [30] was performed. Besides, the misalignment of Z-pins [19,22] may also contribute to the differences between the two sets of experiments.

The experimental assessment of delamination fracture toughness and crack growth rates reported here leads to the conclusion that Z-pins cannot prevent the initiation and growth of

interlaminar crack less than 5mm in length. The crack growth was substantially retarded by Z-pins in WDCB and SLB tests when delamination length became relatively large. In comparison with the mode I and mixed-mode tests, the benefit of Z-pinning for mode II delamination is fairly limited.

4.2 Effect of loading rate

The delamination toughness of unpinned laminates was characterised at two different loading rates here. The influence of loading rate appears to be negligible. Similar results have been reported for other composite material systems from dynamic ELS and DCB tests [36,37]. The delamination response might be expected to change with loading rate, since the yield stress increases and the failure strain decreases with strain rate for epoxy materials [26]. However, it is impossible to exactly quantify the local strain rate at the delamination tip due to the high deformation gradients attained. As illustrated in Fig.3, the opening and sliding displacements were used to evaluate a "nominal" strain rate. Within the investigated dynamic regime, the local strain rate near the initial crack tip was around 100 s^{-1} for dynamic WDCB tests and around 10 s^{-1} for dynamic ENF tests. Higher strain rate may be needed for any strain rate sensitivity of delamination toughness to be observed.

The bridging response of individual Z-pins in mode I & II and mixed-mode delamination have been tested under both quasi-static and dynamic loading rates as reported in [18, 21]. The mode II dominated failure of Z-pins was found to unaffected by the loading rate, while the effectiveness of Z-pins bridging mode I dominated delamination decreased with loading rate. The mode II delamination behaviour of the Z-pinned coupons considered here did not change with loading rate, in terms of both fracture toughness and the crack growth rate. This is consistent with the observations from single pin tests [19,22].

A detailed comparison between Z-pinned WDCB tests and single Z-pin pull-out experiments is shown in Fig.19. As illustrated in Figure.19a, the pull-out displacement rate of Z-pins was very similar for the quasi-static cases. In the dynamic experiments, single Z-pins were pulled out at a speed of approximately 5.5 m/s. In the WDCB tests reported here, the average local pull-out velocity for the pins near crack tip was between 60% and 80% lower. Since the mode I delamination toughness of unpinned laminates was negligible compared to that achieved with TTR, the energy dissipation from single pin tests can be employed to estimate the delamination toughness of Z-pinned laminates for a TTR areal density of 2%. The representative fracture toughness for each type of test is plotted in Fig.19b ,as function of the pin pull-out displacement. Reasonably good agreement can be observed between the single pin tests and the delamination experiments. The trend in rate dependency in the delamination tests is also in agreement with the single pin tests, although significant noise appears in the dynamic WDCB experiments.

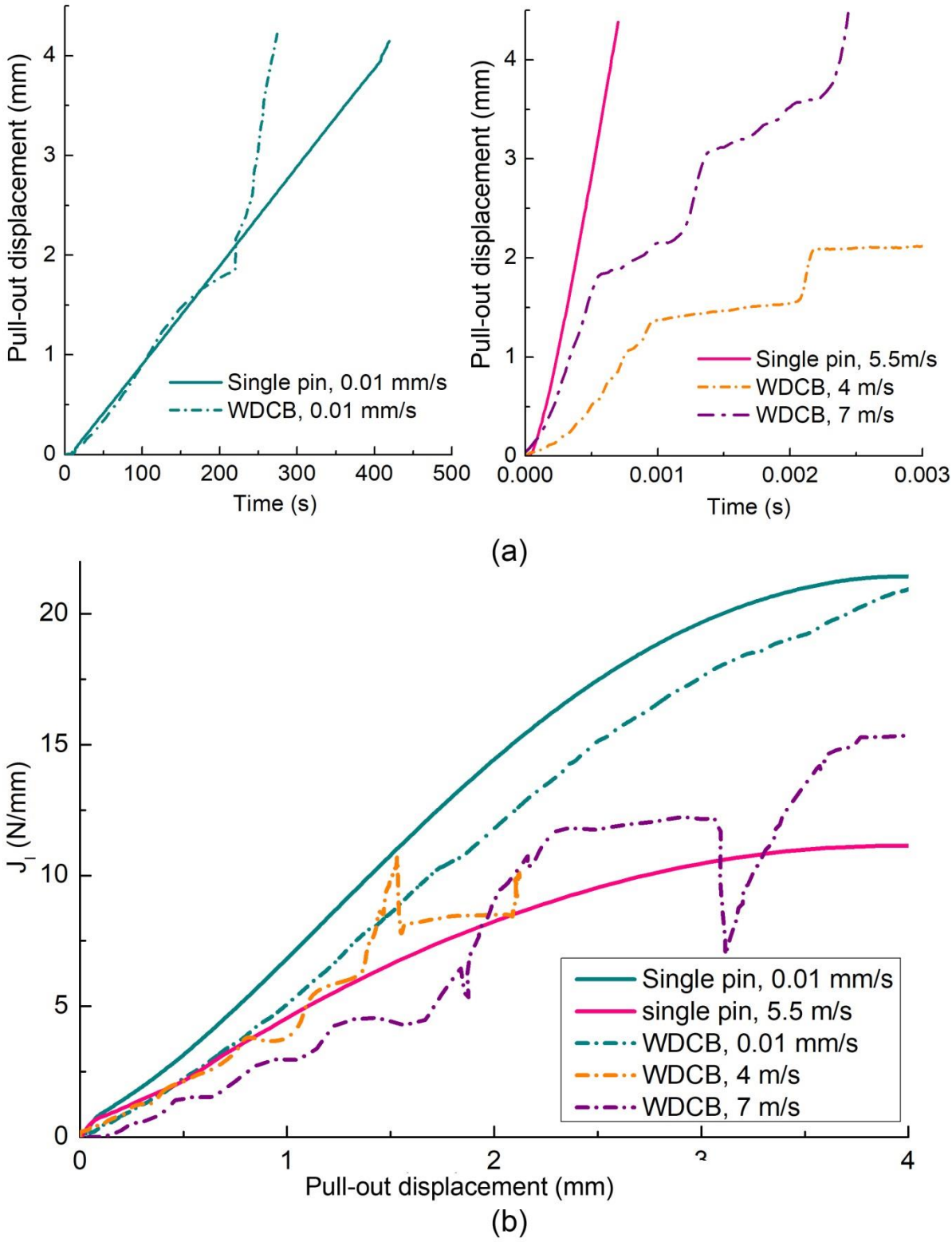

Fig.19 (a) pin pull-out displacement rate in quasi-static tests and dynamic tests; (b) the nominal energy dissipation per unit laminate area as function of pin pull-out displacement

In general, the measurement of applied force posed a significant challenge in all the dynamic experiments. The inertia of the samples resulted in significant oscillation in the measured signal, especially when the coupons were impacted by a flying indenter at constant velocity [16,36,37]. Making use of a rubber sheet as pulse shaper, the indenter that was initially in contact with the sample before the start of the test, applied the displacement with velocity that ramped up smoothly. As shown in this work, the dynamic force-displacement responses were measured with good accuracy. However, due to the gentle ramping up of indenter velocity, the loading rate was not constant and relatively lower compared with the tests that are carried out with flying indenters. Besides, there are steps on the loading rate due to the travelling and reflection of strain pulse within the input bar. New test configurations may be developed in future, for characterizing the delamination fracture toughness at high loading rates.

5. Conclusions

A systematic experimental programme has been conducted to study the dynamic delamination of composite laminates with and without through-thickness reinforcement.

It has been demonstrated that Z-pinning increases the apparent fracture toughness for pure mode I and mixed mode delamination, under both quasi-static condition and at dynamic loading rates. However, the fracture toughness enhancement in mode II due to the insertion of TTR in the form of Z-pins is modest.

It has been also shown that Z-pins are not effective in delaying the initiation of interlaminar cracks or resisting the propagation of relatively short delamination (5 mm long in the case of the experiments reported here). However, further crack growth was

substantially delayed, especially for the WDCB and SLB tests (mode I and mixed-mode conditions).

The mode I delamination toughness of Z-pinned composite laminates exhibited a significant dependency on the loading rate within the range of experimental conditions considered in this paper. This is consistent with previous single pin experiments [19,22].

It has been demonstrated that the fracture toughness of Z-pinned laminates can be evaluated with good accuracy from quasi-static and dynamic test results obtained at single Z-pin level.

6. Acknowledgements

This research is the last part of the project" Understanding Delamination Suppression at High Deformation Rates in Through-Thickness Reinforced Laminated Composites" financially supported by EPSRC funding in the UK (grant no EP/M012905/1). The project has been done collaboratively between University of Oxford, Bristol University and Imperial College London. The authors would like to acknowledge the contribution from industrial partners including Rolls-Royce, BAE Systems, Hexcel and National Composite Centre. The research data are available at https://doi.org/10.17862/cranfield.rd.9118997。

7. References

[1] A.J. Fawcett, G.D. Oakes, Boeing Composite Airframe Damage Tolerance and Service Experience, FAA Work. Compos. Damage Toler. Maintenance, Chicago,. (2006).

[2] S.G. Miller, K.M. Handschuh, M.J. Sinnott, L.W. Kohlman, G.D. Roberts, R.E. Martin, C.R. Ruggeri, J.M. Pereira, Materials, Manufacturing, and Test Development of a Composite Fan Blade Leading Edge Subcomponent for Improved Impact

Resistance, Glenn Research Center, NASA, Cleveland, Ohio, 2015.

[3] M.R. Wisnom, S.R. Hallett, The role of delamination in strength, failure mechanism and hole size effect in open hole tensile tests on quasi-isotropic laminates, Compos. Part A Appl. Sci. Manuf. 40 (2009) 335–342. doi:10.1016/j.compositesa.2008.12.013.

[4] G.A.O. Davies, X. Zhang, Impact damage prediction in carbon composite structures, Int. J. Impact Eng. 16 (1995) 22.

[5] G.A. Schoeppner, S. Abrate, Delamination threshold loads for low velocity impact on composite laminates, Compos. Part A Appl. Sci. Manuf. 31 (2000) 13.

[6] J.P. Hou, N. Petrinic, C. Ruiz, S.R. Hallett, Prediction of impact damage in composite plates, Compos. Sci. Technol. 60 (2000) 9.

[7] S. Abrate, Impact on Laminated Composite Materials, Appl Mech Rev. 44 (1991) 155–190.

[8] Z. Aslan, R. Karakuzu, B. Okutan, The response of laminated composite plates under low-velocity impact loading, Compos. Struct. 59 (2003) 119–127.

[9] M. Nishikawa, K. Hemmi, N. Takeda, Finite-element simulation for modeling composite plates subjected to soft-body, high-velocity impact for application to bird-strike problem of composite fan blades, Compos. Struct. 93 (2011) 1416–1423. doi:10.1016/j.compstruct.2010.11.012.

[10] D.D.R. Cartié, B.N. Cox, N.A. Fleck, Mechanisms of crack bridging by composite and metallic rods, Compos. Part A Appl. Sci. Manuf. 35 (2004) 1325–1336. doi:10.1016/j.compositesa.2004.03.006.

[11] A.P. Mouritz, Review of z-pinned composite laminates, Compos. Part A Appl. Sci. Manuf. 38 (2007) 2383–2397. doi:10.1016/j.compositesa.2007.08.016.

[12] H. Liu, W. Yan, X. Yu, Y. Mai, Experimental study on effect of loading rate on mode I delamination of z-pin reinforced laminates, Compos. Sci. Technol. 67 (2007) 1294–1301. doi:10.1016/j.compscitech.2006.10.001.

[13] I.K. Partridge, D.D.R. Cartié, Delamination resistant laminates by Z-Fiber® pinning: Part I manufacture and fracture performance, Compos. Part A Appl. Sci. Manuf. 36 (2005) 55–64. doi:10.1016/j.compositesa.2004.06.029.

[14] D.D.R. Cartié, J.-M. Laffaille, I.K. Partridge, A.J. Brunner, Fatigue delamination behaviour of unidirectional carbon fibre/epoxy laminates reinforced by Z-Fiber® pinning, Eng. Fract. Mech. 76 (2009) 2834–2845. doi:10.1016/j.engfracmech.2009.07.018.

[15] F. Pegorin, K. Pingkarawat, S. Daynes, A.P. Mouritz, Mode II interlaminar fatigue properties of z-pinned carbon fibre reinforced epoxy composites, Compos. Part A Appl. Sci. Manuf. 67 (2014) 8–15. doi:10.1016/j.compositesa.2014.08.008.

[16] M. Yasaee, G. Mohamed, A. Pellegrino, N. Petrinic, S.R. Hallett, Strain rate dependence of mode II delamination resistance in through thickness reinforced laminated composites, Int. J. Impact Eng. 107 (2017) 1–11. doi:10.1016/j.ijimpeng.2017.05.003.

[17] M. Yasaee, J.K. Lander, G. Allegri, S.R. Hallett, Experimental characterisation of mixed mode traction–displacement relationships for a single carbon composite Z-pin, Compos. Sci. Technol. 94 (2014) 123–131. doi:10.1016/j.compscitech.2014.02.001.

[18] H. Cui, Y. Li, S. Koussios, L. Zu, A. Beukers, Bridging micromechanisms of Z-pin in mixed mode delamination, Compos. Struct. 93 (2011) 11. doi:10.1016/j.compstruct.2011.06.004.

[19] H. Cui, M. Yasaee, G. Kalwak, A. Pellegrino, I.K. Partridge, S.R. Hallett, G. Allegri, N. Petrinic, Bridging mechanisms of through-thickness reinforcement in dynamic mode I&II delamination, Compos. Part A Appl. Sci. Manuf. 99 (2017) 198–207. doi:10.1016/j.compositesa.2017.04.009.

[20] F. Pegorin, K. Pingkarawat, S. Daynes, A.P. Mouritz, Influence of z-pin length on the delamination fracture toughness and fatigue resistance of pinned composites, Compos. Part B Eng. 78 (2015) 298–307. doi:10.1016/J.COMPOSITESB.2015.03.093.

[21] S. Dai, W. Yan, H. Liu, Experimental study on z-pin bridging law by pullout test, Compos. Sci. Technol. 64 (2006) 2451–2457. doi:10.1016/j.compscitech.2004.04.005.

[22] H. Cui, M. Yasaee, S.R. Hallett, I.K. Partridge, G. Allegri, N. Petrinic, Dynamic bridging mechanisms of through-thickness reinforced composite laminates in mixed mode delamination, Compos. Part A Appl. Sci. Manuf. 106 (2018) 24–33. doi:https://doi.org/10.1016/j.compositesa.2017.11.017.

[23] S.A. Ponnusami, H. Cui, B. Erice, M. V Pathan, N. Petrinic, A Wedge-DCB Test Methodology to Characterise High Rate Mode-I Interlami- nar Fracture Properties of Fibre Composites, in: EPJ Web Conf. DYMAT 2018, 2018: pp. 1–6.

[24] ASTM, ASTM D 7905 D7905M - 14. Standard Test Method for Determination of the Mode II Interlaminar Fracture Toughness of Unidirectional Fiber-Reinforced Polymer, n.d. doi:10.1520/D7905.

[25] M.F.S.F.S.F. de Moura, P.M.L.C.L.C. Cavaleiro, F.G.A.A. Silva, N. Dourado, Mixed-mode I+II fracture characterization of a hybrid carbon-epoxy/cork laminate using the Single-Leg Bending test, Compos. Sci. Technol. 141 (2017) 24–31. doi:10.1016/j.compscitech.2017.01.001.

[26] H. Cui, D. Thomson, A. Pellegrino, J. Wiegand, N. Petrinic, Effect of strain rate and fibre rotation on the in-plane shear response of ±45° laminates in tension and compression tests, Compos. Sci. Technol. 135 (2016) 106–115. doi:10.1016/j.compscitech.2016.09.016.

[27] H. Koerber, J. Xavier, P.P. Camanho, High strain rate characterisation of unidirectional carbon-epoxy IM7-8552 in transverse compression and in-plane shear using digital image correlation, Mech. Mater. 42 (2010) 1004–1019. doi:10.1016/j.mechmat.2010.09.003.

[28] M.F.S.F. de Moura, R.D.S.G. Campilho, J.P.M. Gonçalves, Pure mode II fracture characterization of composite bonded joints, Int. J. Solids Struct. 46 (2009) 1589–1595. doi:10.1016/j.ijsolstr.2008.12.001.

[29] C. Materials, Standard Test Method for Mode I Interlaminar Fracture Toughness of Unidirectional Fiber-Reinforced Polymer Matrix Composites 1, 01 (2008).

[30] D7905/D7905M-14, ASTM D7905/D7905M-14, Standard Test Method for Determination of the Mode II Interlaminar Fracture Toughness of Unidirectional Fiber-Reinforced Polymer Matrix Composites, ASTM B. Stand. 15.03 (2014) 1–18. doi:10.1520/D7905.

[31] K. Leffler, K.S. Alfredsson, U. Stigh, Shear behaviour of adhesive layers, Int. J. Solids Struct. 44 (2007) 530–545. doi:10.1016/j.ijsolstr.2006.04.036.

[32] H. Cui, S. Koussios, Y. Li, A. Beukers, Constitutive law of adhesive layer measured with mixed mode bending test, Eng. Fract. Mech. 127 (2014) 235–251. doi:10.1016/j.engfracmech.2014.06.011.

[33] L. Sorensen, J. Botsis, T. Gmür, L. Humbert, Bridging tractions in mode I delamination: Measurements and simulations, Compos. Sci. Technol. 68 (2008) 2350–2358. doi:10.1016/j.compscitech.2007.08.024.

[34] D. Svensson, K.S. Alfredsson, A. Biel, U. Stigh, Measurement of cohesive laws for interlaminar failure of CFRP, Compos. Sci. Technol. 100 (2014) 53–62. doi:10.1016/j.compscitech.2014.05.031.

[35] M.W. Czabaj, J.G. Ratcliffe, Comparison of intralaminar and interlaminar mode I fracture toughnesses of a unidirectional IM7/8552 carbon/epoxy composite, Compos. Sci. Technol. 89 (2013) 15–23. doi:10.1016/j.compscitech.2013.09.008.

[36] M.C. De Verdiere, A.A. Skordos, M. May, A.C. Walton, Influence of loading rate on the delamination response of untufted and tufted carbon epoxy non-crimp fabric composites/Mode II, Eng. Fract. Mech. 96 (2012) 1–10. doi:10.1016/j.engfracmech.2012.05.015.

[37] M. Colin de Verdiere, A.A. Skordos, M. May, A.C. Walton, Influence of loading rate on the delamination response of untufted and tufted carbon epoxy non crimp fabric composites: Mode I, Eng. Fract. Mech. 96 (2012) 11–25. doi:10.1016/J.ENGFRACMECH.2012.05.015.